UNIT-LEVEL AC INDUCED MAGNETIC BEHAVIOR IN THE LOW FREQUENCY REGIME: MEASUREMENT AND CHARACTERIZATION

Sotirios T. Spantideas [(1)], Anastasios E. Giannopoulos [(1)], Anargyros T. Baklezos [(1), (2)], Christos D. Nikolopoulos [(1), (2)], Marco Nicoletto [(3)], Ilario Marziali [(3)], Demis Boschetti [(3)] and Christos N. Capsalis [(1)]

[(1)] School of Electrical and Computer Engineering, National Technical University of Athens, 9 Iroon Polytechniou St., 15780, Greece. Email of corresponding author: sospanti@gmail.com
[(2)] Department of Electronic Engineering, Hellenic Mediterranean University, Romanou 3 Chalepa, 73133, Crete, Greece.
[(3)] Thales Alenia Space Italia - Domain Exploration and Science: Electrical System and EMC, Str. Antica di Collegno 253, 10146, Turin, Italy.

ABSTRACT

In this paper, the measurement and characterization of the unit-level low-frequency induced magnetic response for purposes of magnetic cleanliness is presented. Firstly, we concretely describe the test measurement procedure including the configuration of the measurement setup and the specifications required to accurately obtain the weak induced magnetic signature of a unit. Furthermore, the post-processing pipeline of the measured data for denoising purposes is illustrated through measurements of representative spacecraft equipment (RF Switch unit). Finally, the frequency domain characterization of the induced unit magnetization is performed based on dipole fitting modeling and the induced magnetization tensor is calculated as a linear combination for different orientations of the applied magnetic field.

1. INTRODUCTION

Several space missions have scientific targets that need to adhere to advanced magnetic cleanliness requirements, mainly concerning the temporal variations of the magnetic field emitted by the spacecraft equipment [1]. Depending on the granularity and strictness of the AC magnetic cleanliness requirements, the characterization of equipment in the low regime of the spectrum (below several hundred kHz) should not include only magnetic fields directly emitted from the units that will be placed inside the spacecraft, but shall also take into consideration secondary induced magnetization effects, namely the response of the units to external time-varying magnetic fields [1], [2].

Evidently, each unit inside the spacecraft is in the presence of the magnetic field produced by nearby spacecraft's equipment and, possibly in the presence of external planetary magnetic fields, depending on the mission's scientific target. The time varying induced magnetization typically occurs in cases that the unit enclosure is conducting (eddy currents are generated in response to the external magnetic field) and AC magnetic moments will be generated due to the variations of the external (contribution of the environmental field and the field generated by other equipment) magnetic field [3], [4].

Towards this direction, the AC induced magnetization of units that are included in the spacecraft design are measured by following well-standardized test procedures and requirements [3]. These measurements require extreme level of precision, since in most cases the induced response of a unit generates weak contributions compared to typical magnetic field sources due to avoidance of magnetic materials in the spacecraft design [3]. The obtained unit-level measurement data can be post-processed to estimate a reliable model through simulations that will be able to represent the unit-to-unit interaction and ultimately predict the induced response of a unit in the presence of external magnetic field(s) during the real spacecraft operation.

In the framework of the THOR activity, the scientific objectives of the space mission dictate strict AC magnetic cleanliness requirements ranging from DC up to 250 kHz [2]. The exceptionally low thresholds of the emitted system level AC magnetic field involve also the evaluation of induced magnetization effects due to unit-unit interaction when multiple units located in close proximity operate simultaneously (system or sub-system level integration). While the theoretical framework of the low frequency induced magnetic moment is well-established based on reasonable assumptions [3], the test measurement specifications and the data post-processing required for characterization of the induced behavior are understudied. Hence, this work focuses on the description of the measurement procedure's specifications, as well as the measured data processing, targeting to provide a model for representing the AC induced magnetic field generated by a spacecraft unit.

2. MEASUREMENT SETUP

A representative equipment under test (EUT) selected for characterization of the induced magnetization was a

radiofrequency (RF) Switch (Fig. 1). The RF Switch is considered a unit with relatively small dimensions (approximately 5.3×6×7 cm), being an integral unit of several space missions. During its normal operation, the RF Switch typically exhibits a pulsed magnetic field behavior, involving multiple switch on/offs.

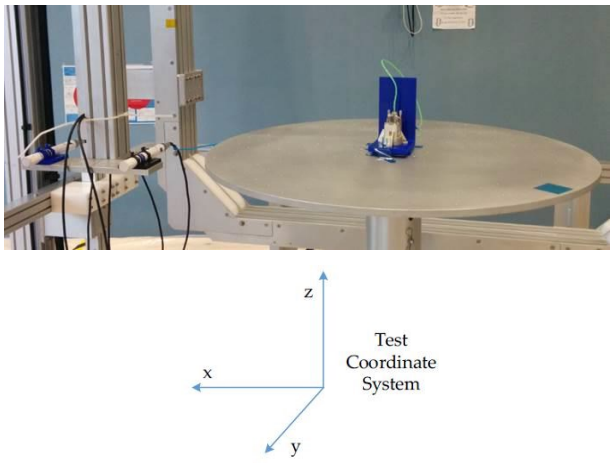

Figure 1. Measurement configuration for AC induced characterization of the RF Switch and Test Coordinate System.

The baseline measurement methodology for the induced response of the EUT can be summarized in the following steps:

- The measurements are performed in the Magnetic Coil Facility (MCF) of TAS-I [5], since rotation of the unit is required to cover its induced field from several orientations and the Helmholtz coils are in charge of providing external magnetic field.
- Two tri-axial fluxgate sensors are used to record the magnetic field time-series in gradiometer configuration, namely with small radial distance between them in order to enable post-processing denoising processes (e.g. discard the environmental background noise).
- The measurement distance of the first sensor is selected around 50 cm for Signal to Noise Ratio (SNR) increment purposes, keeping in mind that the magnetic dipole field follows a $1/r^3$ distance law.
- An external AC magnetic field (10 μT peak to peak) that is spatially uniform in the volume of the EUT is generated with the Helmholtz coils and applied along the vertical z-direction.
- Compensation of environmental magnetic fields (e.g. geomagnetic field) is not required, since the AC magnetic variations of these fields are negligible compared to the applied field.
- Initially, the RF Switch is positioned at the XY plane (Fig. 1) and is rotated in the turntable with a step of 60 degrees, thus obtaining 6 dual measurements.
- The EUT is then flipped (XZ plane and YZ plane) and the above measurement process is repeated for capturing the induced magnetic moment, sequentially along 3 orthogonal axes.
- The AC induced magnetic signature of the unit is obtained for several different frequencies of the applied field (1 Hz and 100 Hz were considered in the present work).
- A background field measurement (in which the unit is removed from the turntable, but the applied field of the coils is still present) is additionally required in order to discard the externally applied field and isolate the AC induced magnetization of the EUT.
- Finally, it should be noted that the tests should be repeated at a different measurement distance in order to verify the validity of the dipole field fall-off ($1/r^3$ distance law)

The measured tri-axial magnetic field data (raw measurements) during the RF Switch AC induced magnetic measurements at 0 degrees for frequency of the externally applied field of 1 Hz are shown in Fig. 2. The raw recordings refer to a 20-sec long measurement window for both magnetic field sensors.

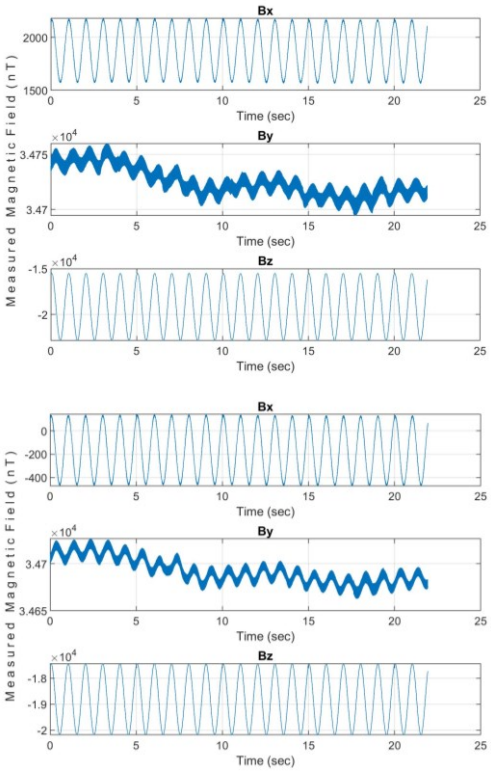

Figure 2. RF Switch AC induced magnetic measurements at 0 degrees – magnetometer 1 (up) and magnetometer 2 (down).

3. DATA POST-PROCESSING

Post-processing of the measured data is required to implement denoising techniques and enable the separation of the induced field from the environmental background variations. For these purposes, the following

post-processing pipeline procedure was sequentially implemented to the measured data:

- Rotation of the measured field components from Magnetometer Coordinate System (MCS) to Test Coordinate System (TCS).
- DC offset removal, since the focus of this work involves the time-varying magnetic field variations and not the significant static component of the geomagnetic field.
- Denoising using the time-domain difference between the two sensors. In principle, the environmental field can be considered spatially uniform at the position of the two fluxgates due to their close proximity.
- Use of notch and/or bandstop filters for suppressing the common operating frequencies of the power network (especially 50 Hz and odd harmonics).

The post-processed time variation of the magnetic field components are depicted in Fig. 3. Evidently, the denoised magnetic field exhibits a sinusoidal shape, as well as a pulsed behavior. It is worth mentioning that these two signal components can be distinguished, i.e. the sinusoidal component is typically due to the applied field of 1 Hz including the response of the RF Switch (related to the conducting parts of the EUT) and the pulsed behavior is due to the normal operation of the EUT (switch on/off).

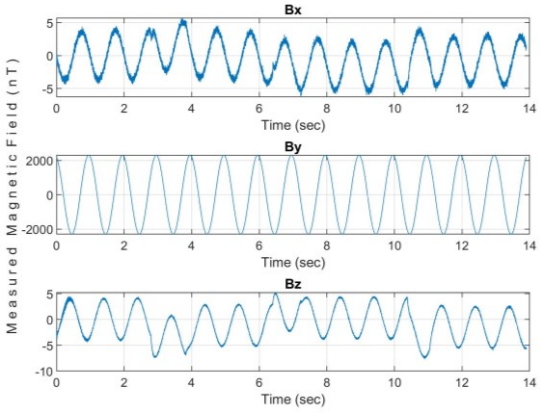

Figure 3. Post-processed magnetic field components at 0 degrees (time-domain difference between the two magnetometers).

Since the AC induced magnetic signature of the unit is expected to emerge at the same frequency with the respective applied magnetic field [4], the deviation between the measured and the applied field (background field measurement without the RF Switch but in the presence of the applied field) can be calculated. According to the test measurement specifications, the position of the magnetometers is maintained fixed during both background and EUT measurements, enabling the estimation of the induced magnetization. Following identical post-processing procedures for the background applied field, the time domain variations of the two signals are compared in Fig. 4, where the windowing function (using hann window) has been applied to both signals.

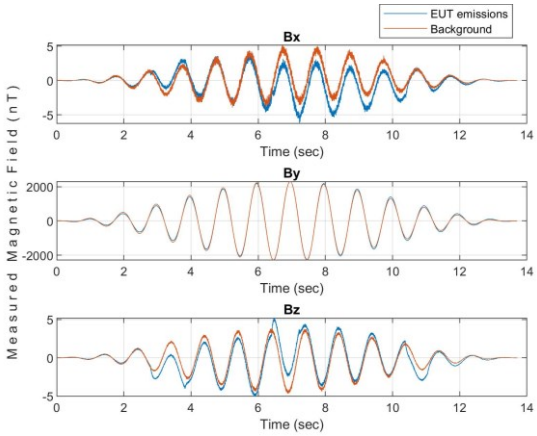

Figure 4. Comparison between the post-processed time domain magnetic field with (blue curve) and without (red curve) the presence of the RF Switch.

The frequency-domain magnetic field components are compared in Fig. 5. As readily observed, the deviation between the two magnetic fields at 1 Hz emerges due to the induced magnetization of the RF Switch. Following the same post-processing procedure, resulting field deviations can be determined for all the rotational measurements in order to cover the induced signature from various orientations, as well as for the other two positioning planes of the unit (XZ and YZ planes).

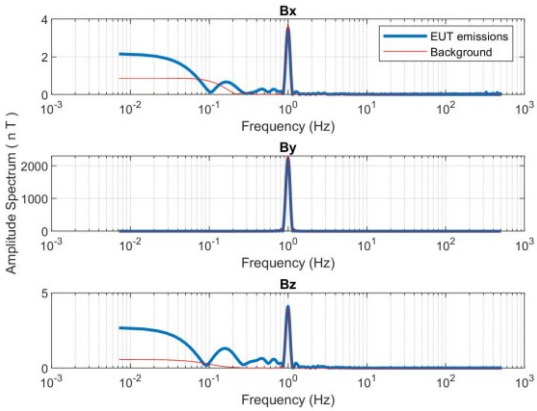

Figure 5. Frequency domain comparison of the magnetic field components with (blue curve) and without (red curve) the presence of the RF Switch.

Similar analysis can be carried out for different frequencies of the applied magnetic field. In the framework of this activity, measurements were also performed for applied field oscillating at 100 Hz. The resulting deviation is shown in Fig. 6 for a single measurement set (0 degrees, XZ orientation). Evidently, the difference between the two magnetic fields at 100Hz

is due to the induced response of the RF Switch.

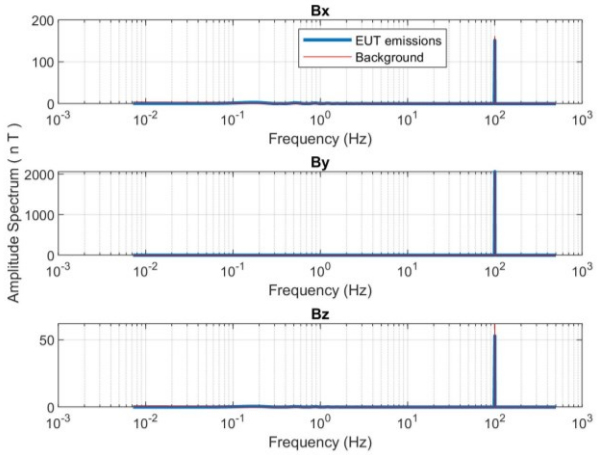

Figure 6. Frequency domain comparison of the magnetic field components with (blue curve) and without (red curve) the presence of the RF Switch. The frequency of the applied field is 100 Hz.

4. MODELING PROCESS

The eddy currents are the physical mechanism for the generation of AC induced magnetic field [4]. However, analytical expression for the induced magnetic dipole moments can be derived in symmetrical cases under several assumptions. Considering that a conducting sphere of radius a (representing the EUT) is located inside a uniform oscillating magnetic field, eddy currents will be formed according to Lenz's Law to oppose the change of flux in the sphere [4]. Since the observation points of interest are located outside of the sphere, the eddy currents give rise to a magnetic moment that depends on the electric and magnetic parameters of the sphere (permittivity ε, permeability μ, and conductivity σ), the radius a, as well as the frequency, the magnitude and the direction of the external magnetic field [1], [4]. In most cases, this theoretical analysis is beneficial for providing insights and simulation results on the magnitude of the induced magnetization. Nevertheless, its implementation can be impractical for real equipment, since conducting parts are not uniformly distributed in the unit surface. In addition, the shape of the EUT is usually quite complex and the AC induced response possibly includes components at all possible directions [3], requiring the specific proposed test measurement procedures.

The focus of the characterization process is to identify a model that accurately describes the AC magnetization of the unit based on the performed measurements, taking also into account the frequency dependency of the induced response. Towards this direction, the induced low frequency magnetic field emissions of the EUT may be modeled with magnetic dipole sources oscillating at the frequency of the external applied field [6]. Assuming a harmonic oscillation for the dipole magnetic moment ($\mathbf{m}(t) = \mathbf{m}e^{-i\omega t}$), where $\omega = 2\pi f$ and f is the frequency of the oscillation, the time varying magnetic field can be expressed:

$$\mathbf{B} = \frac{e^{-i\omega t}\mu_0}{4\pi}\left[\frac{3(\mathbf{r}-\mathbf{r}')[(\mathbf{r}-\mathbf{r}')\cdot\mathbf{m}]}{|\mathbf{r}-\mathbf{r}'|^5} - \frac{\mathbf{m}}{|\mathbf{r}-\mathbf{r}'|^3}\right], \qquad (1)$$

where $\mathbf{r}$ and $\mathbf{r}'$ are the position vectors of the measurement point and the magnetic dipole respectively, and μ_0 is the permeability of free space. Eq. (1) implies a quasi-static nature of the magnetic field, exhibiting the spatial variations identical to the static DC field, while its temporal variations follow the harmonic oscillation of the magnetic moment [6].

In this context, the spatiotemporal magnetic field variations can be distinguished, enabling the monochromatic modeling of the field measurements using the Magnetic Dipole Modeling (MDM) method [7]. The target of the MDM method is to estimate the position $\mathbf{r}'$ and the magnetic moment $\mathbf{m}$ of Eq. (1), based on the measured field $\mathbf{B}$ at measurement points $\mathbf{r}$. The accurate determination of the above parameters requires non-linear inverse operations and is usually performed with stochastic techniques (such as Particle Swarm Optimization, Genetic Algorithms and Differential Evolution) or even Machine Learning methods employing neural networks [8].

For purposes of modeling the induced magnetic signature of the EUT, the Differential Evolution algorithm was used [9]. The algorithm was adapted to process the differential magnetic field, since time domain difference was employed in the data processing (gradio-mode configuration of the sensors). Furthermore, the magnitude values of the post-processed magnetic field, along with the position vectors of the magnetometers were employed to fit the dipole parameters.

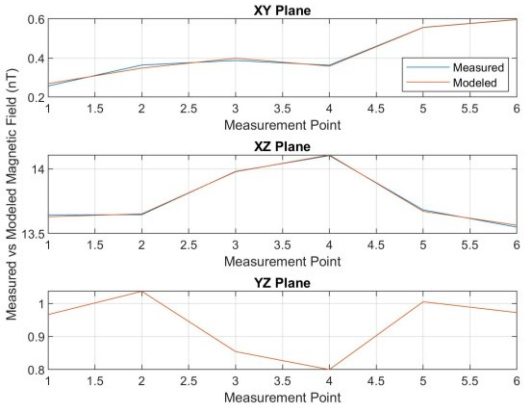

Figure 7. Measured vs modeled magnetic field magnitude for the three orthogonal axes of EUT placement. The frequency of the applied field is 100 Hz.

Indicatively, the measured versus modeled magnitude of the magnetic field are depicted in Fig. 7 for all three orthogonal axes of the EUT placement and for 100 Hz frequency of the applied field. The Root Mean Squared (RMS) error values between the two fields are approximately (0.01, 0.01, 0) nT and the obtained MDM moments in Cartesian coordinates are $(0.02, 0.20, -0.04)$ mAm^2, $(1.33, 0.87, 6.59)$ mAm^2 and $(0.06, -0.15, 0.38)$ mAm^2 for the XY, XZ and YZ planes of EUT placement respectively.

Having obtained the MDM models for all directions of the applied field, the frequency-specific induced magnetic tensor model can be calculated as a linear combination of responses for different orientations of the applied magnetic field:

$$\mathbf{m}_{ind} = \begin{pmatrix} 0.02 & 1.33 & 0.06 \\ 0.20 & 0.87 & -0.15 \\ -0.04 & 6.59 & 0.38 \end{pmatrix} \cdot \begin{pmatrix} \hat{\mathbf{x}} \\ \hat{\mathbf{y}} \\ \hat{\mathbf{z}} \end{pmatrix}, \quad (2)$$

where the unit vectors correspond to the direction of the applied field.

5. CONCLUSIONS

In this present work, test measurement procedures and modeling techniques are presented, targeting to estimate the low frequency induced magnetization of a spacecraft unit. In the framework of the THOR activity, measurement and modeling results are illustrated for a RF Switch and for two frequencies of the applied magnetic field. Since the units inside the spacecraft are in the presence of both AC magnetic field produced by nearby equipment and environmental field variations, the results indicate that their induced response must be additionally included in the analysis if stringent levels of low-frequency magnetic cleanliness are required.

6. ACKNOWLEDGMENTS

The authors would like to express their gratitude to Dr. Axel Junge and Dr. Thomas Voirin for their valuable contribution and fruitful discussions. The measurement procedure and data processing methods has been studied and developed in the framework of Pre-Verification of THOR Electro- Magnetic Cleanliness Approach.

7. REFERENCES

1. Pudney, M., King, S., Horbury, T., Maksimovic, M., Owen, C. J. & Laget, P. (May 2019). Solar orbiter strategies for EMC control and verification. In *IEEE 2019 ESA Workshop on Aerospace EMC (Aerospace EMC),* Budapest, Hungary, pp. 1-6.

2. Capsalis, C.N., Nikolopoulos, C.D., Spantideas, S.T., Baklezos, A.T., Chatzineofytou, E.G., Koutantos, G.I., Boschetti, D., Marziali, I., Nicoletto, M., Tsatalas, S. & Mehlem, K. (May 2019). EMC assessment for Pre-Verification of THOR mission electromagnetic cleanliness approach. In *IEEE 2019 ESA Workshop on Aerospace EMC (Aerospace EMC),* Budapest, Hungary, pp. 1-6.

3. ESA. (2012). Space Engineering: Electromagnetic Compatibility Handbook. *ECSS-E-HB-20-07A, Eur. Space Agency, ESA-ESTEC*, Noordwijk, The Netherlands. http://everyspec.com/ESA/ECSS-E-HB-20-07A_47799/

4. Bidinosti, C.P., Chapple, E.M. & Hayden, M.E. (2007). The sphere in a uniform RF field-Revisited. *Concepts in Magnetic Resonance Part B: Magnetic Resonance Engineering: An Educational Journal*, *31*(3), 191-202.

5. Cucca, M., Marzot, M., Del Prete, A., Leone, A., & Ferrari, E. (2019, May). Enhanced Magnetic Coil Facility for Magnetic Cleanliness, Characterization and Susceptibility. In *2019 ESA Workshop on Aerospace EMC (Aerospace EMC)* (pp. 1-6). IEEE.

6. Jackson, J.D. (1999). *Classical Electrodynamics.* New York, John Wiley and Sons.

7. Junge, A., & Marliani, F. (2011, August). Prediction of DC magnetic fields for magnetic cleanliness on spacecraft. In *2011 IEEE International Symposium on Electromagnetic Compatibility* (pp. 834-839). IEEE.

8. Spantideas, S.T., Giannopoulos, A.E., Kapsalis, N.C., & Capsalis, C.N. (2021). A Deep Learning Method for Modeling the Magnetic Signature of Spacecraft Equipment Using Multiple Magnetic Dipoles. *IEEE Magnetics Letters*, *12*, 1-5.

9. Qin, A. K., Huang, V. L., & Suganthan, P. N. (2008). Differential evolution algorithm with strategy adaptation for global numerical optimization. *IEEE transactions on Evolutionary Computation*, *13*(2), 398-417.